Density functional calculations on the structure of crystalline polyethylene under high pressures

M. S. Miao, M.-L. Zhang, V. E. Van Doren, C. Van Alsenoy, and José Luís Martins

Citation: The Journal of Chemical Physics **115**, 11317 (2001); doi: 10.1063/1.1420404
View online: http://dx.doi.org/10.1063/1.1420404
View Table of Contents: http://scitation.aip.org/content/aip/journal/jcp/115/24?ver=pdfcov
Published by the AIP Publishing

Density functional calculations on the structure of crystalline polyethylene under high pressures

M. S. Miao,[a] M.-L. Zhang, and V. E. Van Doren
Department of Physics, University of Antwerp (RUCA), Groenenborgerlaan 171, B-2020 Antwerpen, Belgium

C. Van Alsenoy
Department of Chemistry, University of Antwerp (UIA), Universiteitsplein 1, B-2610 Antwerpen, Belgium

José Luís Martins
Instituto de Engenharia de Sistemas e Computadores, Rua Alves Redol 9, 1000-029 Lisboa, Portugal and Departmento de Física, Instituto Superior Técnico, Av. Rovisco Pais, 1049-001 Lisboa, Portugal

(Received 3 August 2001; accepted 2 October 2001)

The geometrical structures of the crystalline polyethylene under several different external pressures up to 10 GPa are optimized by a pseudopotential plane wave density functional method. Both local density (LDA) and generalized gradient (GGA) approximations for exchange-correlation energy and potential are used. It is found that LDA heavily underestimate the geometry parameters under ambient pressure but GGA successfully correct them and get results in good agreements with the experimental geometry. The calculated GGA volume is about 94 $Å^3$ in comparison with the x-ray scattering value of about 92 $Å^3$ and the neutron scattering value of 88 $Å^3$. The bulk and Young's modulus are calculated by means of several different methods. The Young's modulus along the chain ranges from about 350 to about 400 GPa which is in good agreement with the experimental results. But the bulk modulus is several times larger than those of experiments, indicating a different description of the interchain interactions by both LDA and GGA. The band structures are also calculated and their changes with the external pressure are discussed. © *2001 American Institute of Physics.* [DOI: 10.1063/1.1420404]

I. INTRODUCTION

The role of polyethylene in polymer science is perhaps comparable with the role of silicon in solid state physics and the role of hydrogen in atomic physics. Due to its structural simplicity and its technological importance,[1] many probes have been applied to polyethylene together with many concurrent theoretical studies.

Previous theoretical studies on polyethylene as well as the other polymers were mostly done for a single chain by utilizing the one-dimensional periodicity of the system.[2,3] The methods ranged from semiempirical[4–10] to first principles[11–15] and in some cases including correlation effects from many body perturbation theory.[16,17] In recent years, density functional (DFT) method were also applied to single chain polymer system including polyethylene.[18–20] In our previous work,[21] the conformational and the electronic structure of a single chain polyethylene were calculated at ten different dihedral angles using both Gaspar–Kohn–Sham exchange and Perdew–Zunger correlation energy and potentials.

Several DFT studies have been done on crystalline polymer systems. Vogl *et al.*[22] reported a local density approximation (LDA) calculation of crystalline *trans*-polyacetylene. The geometry of the crystalline state of another well studied conducting polymer polyparaphenylene were optimized by a pseudopotential plane wave method and its electronic structure was obtained by a full potential linearized augmented plane wave method (LAPW).[23] Recently, the geometry and the electronic structures of crystalline polyethylene under the ambient pressure were studied by Montanari *et al.* using pseudopotential plane wave methods with both the LDA and generalized gradient approximation (GGA) exchange-correlation energy.[24] They concluded that the LDA overestimates the binding energies between the chains and the GGA calculations lead to no interchain binding at all. Using the similar method but only with LDA exchange-correlation potential, Hageman *et al.* studied the elastic modulus as well as the band structure of crystalline polyethylene.[25,26]

In this paper, the geometrical structure as well as the elastic modulus of crystalline polyethylene under several different pressures are studied by a pseudopotential plane wave method with both LDA and GGA exchange-correlation contribution. The details of the electronic structure calculations and the structural optimization as well as the dimensions used will be described in Sec. II. Section III presents the optimized geometry under ambient pressure. The Young's modulus is calculated from elastic constants in Sec. IV. Section V present the geometries under high pressure. The equation of state and bulk modulus are also obtained. The electronic structure and its changes with the external pressure will be presented in Sec. VI. And finally, the results will be summarized and discussed in Sec. VII.

[a]Present address: Department of Physics, Case Western Reserve University, Cleveland, Ohio 44106-7079.

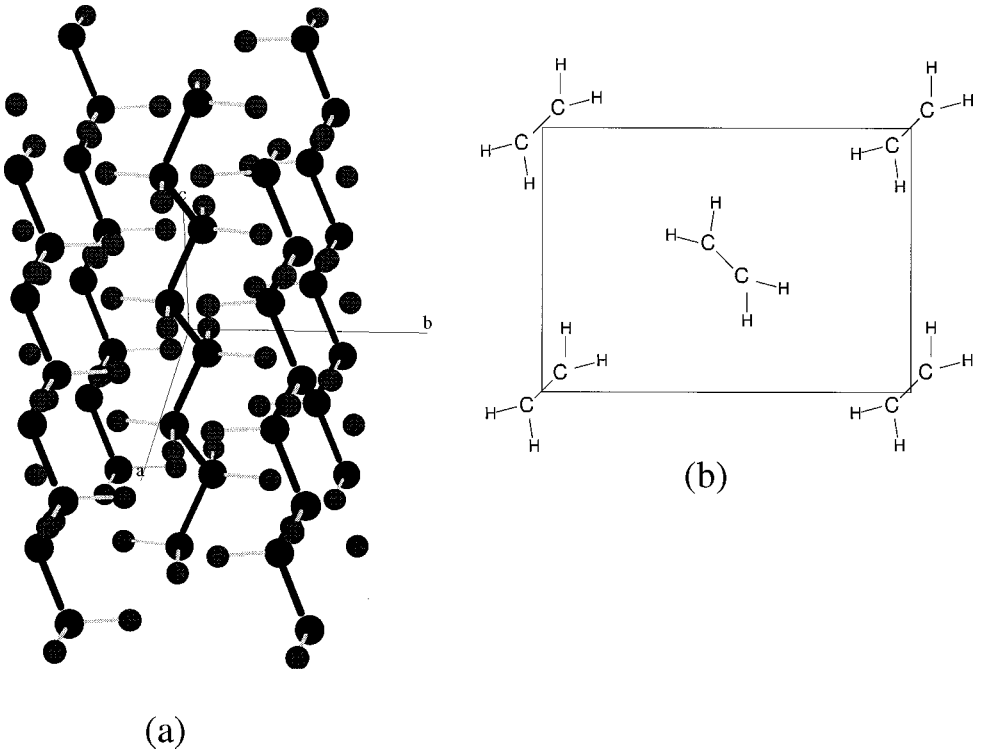

FIG. 1. Crystalline structure of polyethylene. (a) Side-view of orthorhombic structure of polyethylene. (b) Projection of unit cell on the *ab* plane.

II. METHODS AND THE CALCULATIONAL PROCEDURE

The structural optimization in this article is based on a modified variable-cell-shape (VCS) (Ref. 27) dynamics which considers changes in both the positions of the ions and the components of the metric (the dot products between the lattice vectors of the simulation cell). A conjugated gradient method, Davidon algorithm, is used to relax the positions of the atoms and to determine the lattice vectors. Instead of the total energy E, the enthalpy $H=E+PV$ is minimized at different external pressures of 0, 2, 4, 6, 8, and 10 GPa. The total energy is obtained by self-consistently solving the Kohn–Sham equation for the electron state with a Ceperley–Alder[28] correlation potential as parameterized by Perdew–Zunger[29] or with a Perdew–Burke–Ernzerhof GGA.[30] The interaction of the valence electrons with the core electrons are described by an *ab initio* norm-conserving pseudopotential.[31] The electronic wave functions are expanded in terms of a plane-wave basis set. The core radius of carbon pseudopotential is chosen to be 1.30 a.u. and the full Coulomb potential is used for hydrogen. A cutoff energy of 80 Ry is used to obtain convergence of the total energy with respect to basis set size, corresponding to about 8000 plane waves. The Brillouin zone integrations are done with 3 special *k*-points for LDA and 8 for GGA.

In a general procedure of optimization, the symmetry of the molecular crystal may not be preserved because of accumulation of numerical inaccuracies. In our case, we impose the condition that the initial symmetry is preserved. Otherwise we perform an unconstrained minimization of the enthalpy with respect to all the variables that are independent by symmetry. (See Ref. 32 for the details.)

III. GEOMETRIES UNDER ZERO PRESSURE

Polyethylene crystallizes in an orthorhombic structure with space group *Pnam* (Ref. 1) (see Fig. 1). In each unit cell, there are four $(CH)_2$ groups situated in two polymer chains. The LDA and GGA optimized geometrical parameters, including the bond lengths, the bond angles and the setting angle of the chain as well as the lattice vectors are listed in Table I together with the experimental results[33–35] and the other theoretical predictions[36,37,21,24] for both the single chain and the crystalline system. For reasons of numerical stability that will be discussed below, the GGA geometry is actually obtained at a pressure of 0.1 GPa which is sufficiently small in comparison with the pressure steps of 2 GPa used in this article. According to the results in next two sections concerning with the pressure dependence of the parameters, the changes of intrachain geometries caused by this imposed pressure is negligible and the changes of the interchain parameters is about 0.5%. A simulated single chain calculation is performed by setting the chains in a simple orthorhombic lattice with very large lattice constants using the same plane wave method. The GGA geometry for this simulated single chain is also listed in Table I. In that table we verify that LDA grossly underestimates the interchain distances and the lattice constants, but that GGA corrects most of the LDA deficiencies and predicts interchain parameters and the cell volume in good agreement with the x-ray[33,34] and neutron[35] scattering results. Both GGA and LDA give good results for intrachain geometry, the errors being smaller than a few percent. The fact that LDA underestimates the intermolecular distances, but gives good in-

TABLE I. The optimized geometrical parameters in comparison with the x-ray and neutrons scattering experimental and the previous Hartree–Fock (HF) and density functional (DFT) calculational results. d is the shortest distances between the hydrogen atoms and between the carbon atoms. ϕ, the setting angle, is the angle between the PE chain plane and the ac plane. All the bond lengths, the atom distances, and the lattice vectors are in Å and all the angles are in deg. The results in the first two columns are from this work with GGA and LDA exchange-correlation potential and the results in the third column are for isolated chain simulated by using very large lattice constants.

	GGA	LDA (CA)	GGA (chain)	X ray[a]	X ray[b]	Neutrons (4 K)[c]	Neutrons (90 K)[c]	HF[d]	HF[e]	DF (chain)[f]	DFT (crystal)[g]
Bond length											
r_{C-C}	1.53	1.50	1.54	1.53	1.527	1.578(5)	1.574(5)	1.536	1.541	1.515	1.512
r_{C-H}	1.11	1.12	1.11	⋯	1.091	1.06(1)	1.07(1)	1.083	1.087	1.10	1.111
Bond angles											
CCC	113.53	113.50	114.16	112	112±0.8	107.7(5)	108.1(5)	112.7	112.5	113.0	114.3
HCH	106.06	105.43	105.94	⋯	⋯	109.0(1)	110.0(1)	106.8	107.2	109.7	105.2
Setting angle											
ϕ	44.14	44.44	⋯	48.8	45	41(1)	41(1)	⋯	⋯	⋯	41.3
Distances											
$d_{C\cdots C}$	4.13	3.66		4.13	4.59	⋯	⋯	⋯	⋯	⋯	3.67
$d_{H\cdots H}$	2.64	2.08		⋯	⋯	⋯	⋯	⋯	⋯	⋯	⋯
Lattice constants											
a	7.304	6.549	⋯	7.40	7.388	7.121	7.161	⋯	⋯	⋯	6.73
b	5.017	4.446	⋯	4.93	4.929	4.851(1)	4.866(2)	⋯	⋯	⋯	4.53
c	2.565	2.515	⋯	2.543	2.539	2.548(1)	2.546(1)	⋯	⋯	⋯	2.52
Volume											
V	93.97	73.24		92.77	92.46	88.02	88.72				

[a] Reference 33.
[b] Reference 34.
[c] Reference 35.
[d] Reference 36.
[e] Reference 37.
[f] Reference 21.
[g] Reference 24.

tramolecular distances, while GGA gives reasonable values for both intra and intermolecular distances is the usual trend for first row molecular crystals.

We also optimized the geometry parameters with other parametrizations of the exchange-correlation energies and potentials, including the Hedin–Lundqvist (HL), and Wigner (WI). The three different LDA exchange-correlation functionals, CA, HL, and WI, predict very similar geometries for polyethylene crystals under zero pressure. Their optimized volumes are 73.23 Å^3, 73.24 Å^3, and 76.67 Å^3, respectively, and the differences between the C–C bond length are within 0.01 Å. We find the usual result that the differences between CA and HL are minute, and that WI gives slightly larger lattice constants. In our previous DFT calculations on the single chain polyethylene[21] where we found that the Gaspar–Kohn–Sham (GKS) and the Perdew–Zunger optimized C–C bond lengths are different from each other for about 0.02 Å.

It was found previously,[24] that LDA predicts a well defined minimum of the total energy as a function of volume, whereas a GGA calculation shows no minimum. With LDA we obtain a large binding energy of 0.44 eV per unit cell, in good agreement with the value for LDA reported previously.[24] However for the case of GGA, we find a much flatter energy surface. At the experimental interchain distance we find a very small repulsive energy of 0.01 eV, whereas in that previous calculation a repulsive energy of about 0.2 eV can be read from the figures. Furthermore our automatic geometry optimization did converge to a geometry close to the experimental value, suggesting a local minima, or at least a region with a very flat energy surface. We performed a series of tests for both the crystal polyethylene and isolated chains, using larger cutoffs (120 Ry), more k points (8–16), tried using the partial core corrections for the carbon pseudopotential, but did not find a change in behavior. Montanari and Jones[24] used a method similar to ours, except for the use of the Becke–Perdew[38,39] GGA instead of the PBE (Ref. 30) GGA so the difference in behavior should be traced to the use of a different GGA prescription. The interactions that bind the chains include the dispersion forces and also a small attractive electrostatic interactions. Notice that both LDA and GGA neglect the dispersion force that dominate the bonding between the chains at large distances. One should not expect accurate results for weakly bonded systems, that seems to be the case of polyethylene.

To avoid the uncertainties related to a very flat energy surface, we decided to use a pressure of 0.1 GPa for the lowest pressure GGA calculations. At that pressure the lattice constants are almost identical to the values obtained at 0 GPa. The most significant changes are for the setting angle ϕ and the H–H distance. And they are all less then 1%. Using the experimental bulk moduli, such a pressure should change the lattice constants by around 1%, which is within the expected accuracy of DFT.

IV. YOUNG'S MODULUS

Since the polyethylene crystal is formed by the polymer chains, it is highly anisotropic. To determine its mechanical properties under high pressure, we must calculate several elastic moduli, such as the Young's moduli along and perpendicular to the chain.

For an orthorhombic system, there are nine independent elastic constants, namely,

$$C_{11}, C_{22}, C_{33}, C_{12}, C_{13}, C_{23}, C_{44}, C_{55}, C_{66},$$

in which only the first six are needed for calculating the Young's modulus and bulk modulus. The relation between the external diagonal stress and the diagonal components of the strain tensor can be expressed as the following matrix equation:

$$\begin{pmatrix} C_{11} & C_{12} & C_{13} \\ C_{12} & C_{22} & C_{23} \\ C_{13} & C_{23} & C_{33} \end{pmatrix} \begin{pmatrix} \eta_1 \\ \eta_2 \\ \eta_3 \end{pmatrix} = \begin{pmatrix} P_1 \\ P_2 \\ P_3 \end{pmatrix} \tag{1}$$

in which $\eta_i (i=1,2,3)$ is the diagonal components of the strain tensor and P_i is those of the stress tensor. To obtain Young's modulus along the chain, one needs to solve η_3 at the condition of $P_1=P_2=0$ GPa and $P_3=1$ GPa. The solution is easy to get by solving the above linear algebra equation,

$$Y_z = \frac{1}{\eta_3}\bigg|_{P_1=P_2=0,P_3=1} = \frac{\begin{vmatrix} C_{11} & C_{12} & C_{13} \\ C_{12} & C_{22} & C_{23} \\ C_{13} & C_{23} & C_{33} \end{vmatrix}}{\begin{vmatrix} C_{11} & C_{12} \\ C_{12} & C_{22} \end{vmatrix}} \cong C_{33} - \frac{C_{23}^2}{C_{22}} - \frac{C_{13}^2}{C_{11}}. \tag{2}$$

Two different methods to calculate the elastic constants from the first principle simulations are used. The linear dependent of the stress on strain are assumed for both methods. In one method, the total energies are calculated for a structure with lattice constants deformed from the stable structure. The elastic constants are calculated from the second derivatives of the total energy versus the deformation,

$$C_{ij} = C_0 \frac{U(\eta_i) + U(\eta_j) - 2U(0)}{\eta_i \eta_j} \frac{1}{V}. \tag{3}$$

U is the total energy for the equilibrium and the deformed lattices. If Hartree is used as the unit for energy, $C_0 = 4.359\,784\,2 \times 10^9$ GPa Å^3 Hartree^{-1}. In the second method, the stresses are calculated directly from the deformed structure using the Nielson–Martin stress theorem[40,41] and its generalization to include the stress of GGA. The exchange-correlation parts of the stress is

$$\sigma_{\alpha\beta} = \delta_{\alpha\beta}[\epsilon_{\rm xc}(\rho(r)) - \mu_{\rm xc}(\rho(r))]\rho(r) \tag{4}$$

for LDA and

$$\sigma_{\alpha\beta} = \delta_{\alpha\beta}[\epsilon_{\rm xc}(\rho(r), \nabla\rho(r)) - \mu_{\rm xc}(\rho(r))]\rho(r) - \frac{\partial[\rho(r)\epsilon_{\rm xc}(\rho(r), \nabla\rho(r))]}{\partial(\partial_\beta \rho(r))} \frac{\partial\rho(r)}{\partial r_\alpha} \tag{5}$$

for GGA.[42]

Table II lists all the calculated GGA and LDA elastic constants and the corresponding Young's Modulus using the above two methods. Generally, the two methods obtain similar results especially for the diagonal elastic constants. Large differences appears for the off-diagonal elastic constants of GGA, which may due to numerical noise in the determination of those small coefficients. According to formula (2), the Young's modulus is mainly determined by the diagonal elastic constants since the off-diagonal ones are very small in comparison. The modulus Y_z is the Young's modulus along the polymer chain. For comparison, our calculated LDA and GGA Young's modulus with the previous theoretical[16,26,43–47] and experimental[48–51] results are listed in Table III. Generally, the theoretical modulus are 10%–20% larger than the experimental modulus. Both GGA and the LDA give Young's modulus along the polymer chains in good agreement with the experimental results and the previous single chain and the crystalline calculations. In general GGA gives smaller elastic constants and the Young's modulus. The very large modulus obtained by the semiempirical method and the HF method with small basis are reduced evidently by using large Basis and further on by counting the correlation effects to second order perturbation (MP2). The GGA modulus are close to the HF results using the large basis.

TABLE II. The calculated elastic constants and Young's modulus. All the results are in GPa. The numbers in the parentheses denote the first and the second way to calculate the elastic constants from a manually deformed structure.

	C_{11}	C_{22}	C_{33}	C_{12}	C_{13}	C_{23}	Y_X	Y_Y	Y_Z
LDA(I)	41.18	47.14	405.78	11.25	3.19	6.50	38.49	43.99	404.81
LDA(II)	48.06	44.22	375.19	12.21	1.43	6.20	44.69	41.03	374.32
GGA(I)	39.2	32.86	347.85	2.46	4.67	2.35	38.96	32.69	347.16
GGA(II)	32.05	30.95	389.27	18.74	5.89	5.21	20.68	19.98	388.03

TABLE III. Comparison of the calculated and the experimental Young's modulus. The results include our GGA and LDA and a previous LDA modulus for crystalline polyethylene, previous HF, and LDA calculations for single chain or cluster polyethylene as well as the experimental measurements. For the denotation of GGA and LDA methods, see the caption in Table II.

	Young's modulus (GPa)
Crystalline polyethylene	
GGA(I) (this work)	347.16
GGA(II) (this work)	388.03
LDA(I) (this work)	374.32
LDA(II) (this work)	404.81
LDA(Hageman *et al.* 1998)[a]	366
Single chain polyethylene	
MNDO-CO (Dewar *et al.* 1979)[b]	493.5
HF/STO-3G MO (Brower *et al.* 1980)[c]	420±30
HF/6-31G CO (Suhai, 1983)[d]	339
HF/6-31G CO+MP2 (Suhai 1983)[d]	303
HF/6-31G*+MP2 (Crist *et al.* 1996)[e]	336
DFT/(7111/411/1*) (M. L. Zhang *et al.* 1999)[f]	320–360
HF/MO clusters (A. Peeters, 1999)[g]	276, 356
Experimental results	
X-ray diffraction (Sakurada *et al.* 1962)[h]	235–255
Inelastic neutron scattering (Feldkamp *et al.* 1968)[i]	239
Raman spectroscopy (Schaufele, 1967)[j]	358
IR vibrational analysis (Barham, 1979)[k]	257–340

[a]Reference 26.
[b]Reference 43.
[c]Reference 44.
[d]Reference 16.
[e]Reference 45.
[f]Reference 46.
[g]Reference 47.
[h]Reference 48.
[i]Reference 49.
[j]Reference 50.
[k]Reference 51.

TABLE IV. The LDA geometry parameters vs the external pressure, from 0 GPa to 10 GPa. For the denotations and the units, see the caption of Table I.

	0 GPa	2 GPa	4 GPa	6 GPa	8 GPa	10 GPa
Bond length						
r_{C-C}	1.504	1.500	1.496	1.492	1.489	1.486
r_{C-H}	1.111	1.110	1.107	1.106	1.106	1.105
Bond angles						
CCC	113.50	113.42	113.26	113.11	113.05	113.05
HCH	105.43	105.37	105.22	105.12	105.08	105.09
Setting angle						
ϕ	44.44	43.38	43.32	43.66	43.65	43.56
Distances						
$d_{C\cdots C}$	3.66	3.54	3.46	3.45	3.35	3.31
$d_{H\cdots H}$	2.08	1.99	1.93	1.88	1.85	1.81
Lattice constants						
a	6.549	6.339	6.196	6.092	6.007	5.943
b	4.446	4.313	4.224	4.152	4.092	4.036
c	2.515	2.506	2.498	2.491	2.485	2.479
Volume						
V	73.24	68.51	65.38	63.01	61.08	59.46

V. EQUATION OF STATE AND BULK MODULUS

The LDA and GGA optimized geometry under different pressures are shown in Tables IV and V, respectively. As expected, the geometrical parameters between the chains such as the C–C distance between neighboring chains and the lattice constants changes rapidly with increasing external pressure in comparison with the bond lengths and the bond angles within a polymer chain. As expected, a strong anisotropic effect of the pressure is revealed by the changes of the lattice constants along different directions. This coincides with the changes of the inter- and intramolecular distances. For example, the interchain C–C distance decreases for almost 10%, whereas the C–C bond length shows almost negligible changes. The deformation along the *c* direction is contributed by the changes of the bond length and the bond angles of the backbone carbon. Both changes are not more than 1%.

TABLE V. The GGA geometry parameters vs the external pressure, from 0 GPa to 10 GPa. For the denotations and the units, see the caption of Table I.

	0 GPa	2 GPa	4 GPa	6 GPa	8 GPa	10 GPa
Bond length						
r_{C-C}	1.512	1.506	1.498	1.497	1.495	1.493
r_{C-H}	1.110	1.101	1.093	1.095	1.092	1.089
Bond angles						
CCC	113.53	113.11	114.03	113.50	113.32	113.21
HCH	106.06	105.55	105.11	105.43	105.47	105.23
Setting angle						
ϕ	41.14	42.76	42.60	45.62	48.26	46.75
Distances						
$d_{C\cdots C}$	4.13	3.96	3.77	3.58	3.46	3.43
$d_{H\cdots H}$	2.64	2.35	2.20	2.05	1.97	1.96
Lattice constants						
a	7.304	7.102	6.775	6.416	6.194	6.167
b	5.017	4.727	4.534	4.346	4.251	4.143
c	2.565	2.514	2.512	2.504	2.499	2.492
Volume						
V	93.97	84.39	77.16	70.11	65.79	63.67

TABLE VI. Bulk modulus obtained by fitting equation of state to a polynomial. An experimental and a molecular simulation results are listed together.

	PE(LDA)	PE(GGA)	PE(Expt[a])	PE(MS[b])
V	73.23	93.90		
a_1	−2.2566	−5.233		
a_2	0.33333	0.3414		
a_3	−0.02712	−0.03232		
B_0	25.0319	17.93	5.6	11.1(static)
				9.8($T=0$)
B_0'	4.70393	1.338	7.0	7.2(static)
				7.2($T=0$)
B_0''	0.97937	1.04		

[a]Reference 52.
[b]Reference 53.

By fitting the volume to a polynomial of the pressure P, the bulk modulus as well as its pressure derivatives relate to the fitting coefficients in the following way:

$$a_1 = -\frac{V_0}{B_0}, \quad a_2 = \frac{1+B_0'}{2B_0^2} V_0. \tag{6}$$

The bulk modulus can also be obtained by assuming a hydrostatic pressure ($P_1=P_2=P_3=1$) and solving the corresponding strain components from Eq. (1) and expressing the bulk modulus as

$$B_0 = (\eta_x + \eta_y + \eta_z)^{-1}. \tag{7}$$

The results for the bulk modulus and its pressure derivative are given in Table VI in comparison with the experimental results[52] and the previous theoretical calculations.[53] From Table VI, it can be seen that the calculated bulk modulus is about four times larger than the experimental value and its pressure derivative is smaller. This large difference could be caused by the amorphous nature of the experimental material but we cannot rule out a deficiency of the exchange-correlation potential. Combining with the results on Young's modulus, it can be concluded that despite of the very good results on Young's modulus along *c* axis concerning with the interactions within the chain, both GGA and LDA show large disagreements to experimental results on Bulk modulus which has large components of the interchain interactions. In summary GGA gives good geometry but it is difficult to quantify it on describing the interchain interactions yet (Table VII).

VI. BAND STRUCTURE

Several DFT band structures of polyethylene have been reported previously for both the single chain as well as the crystalline polyethylene. In this article, both LDA and GGA bands are calculated. Figure 2 plots the LDA and GGA bands for crystalline polyethylene with optimized geometries under 0 GPa and 6 GPa external pressures. The band characteristics including band gap between the valence and the conduction bands as well as the valence bandwidths are listed in Table VIII.

In general, the GGA and LDA valence bands are similar to each other for both the results of 0 GPa and 6 GPa except that LDA bands have larger dispersions in both directions

TABLE VII. Comparisons of the GGA and LDA bulk modulus calculated in this work and the experimental as well as a molecular simulation results. For the denotation of GGA and LDA methods, see the caption of Table IV.

	B_0 (GPa)
GGA(I)	18.39
GGA(II)	24.5
LDA(I)	27.52
LDA(II)	26.37
GGA(fitting)	17.93
LDA(fitting)	25.03
MS(static)[a]	11.1
MS($T=300$ K)[a]	7.0
Expt.[b]	5.6

[a]Reference 53.
[b]Reference 52.

parallel to and perpendicular to the chain direction. Large differences are found for the conduction bands, indicating the deficiency of the Kohn–Sham exited states which does not have any clear physical meaning by its definition. The valence bands form two groups. The lowest-lying bands are typically associated to carbon $2s$ σ bonding between backbone carbons whereas the upper bands associated with carbon-hydrogen σ bands. For the symmetry of the bands, see Ref. 21.

The calculated band gaps are 6.2 eV for GGA and 6.7 eV for LDA under 0 GPa. The corresponding values were obtained to be 5.7 eV and 6.0 eV by Montanari *et al.*[24] In a recent study[21] on single chain polyethylene using Gaussian basis sets, we obtained a 8.0 eV band gap (CA). In comparison with the HF gap[11,12,14,16] the DFT gaps are much smaller, which agrees with the usual trend. Although the DFT gaps for both single chain and crystalline polyethylene are close to the optical gap of 8.8 eV, it can not be concluded that DFT gap values are better because the optical gap is reduced by the exciton effects.

The experimental valence band structure of polyethylene has been derived from angle-resolved photoemission experiments on alkanes, $CH_3(CH_2)_{34}CH_3$.[54,55] So it is worthy to compare the DFT valence bands with this experimental results. The overall forms of GGA and LDA valence bands are both similar to the experimental form and the previous band structure calculations.[20,21,24] Both GGA and LDA total valence band widths are in reasonable agreements with experimental and previous theoretical results. GGA gives better low-lying band width and the gap between two groups of valence bands, whereas LDA overestimates the former and underestimates the latter values.

LDA results show larger coupling of the bands of the neighboring chains in $\Gamma-Z$ and $U-X$ directions and larger dispersions in $\Gamma-Y$, which coincides the larger binding energy of the neighboring chains for LDA. The GGA band dispersion for the occupied state of most H character is 0.77 eV, corresponding to a nearest neighboring interaction of 0.39 eV. The LDA dispersion is 1.73 eV, corresponding the interchain interaction of 0.87 eV. A dispersion of 1.24 eV was obtained by Hageman *et al.*[26]

For studying the pressure effects on the band structure, the GGA and the LDA band structures are calculated for crystalline polyethylene under 6 GPa external pressure. As expected, the coupling of the bands in $\Gamma-Z$ and $U-X$ directions and the dispersions along $\Gamma-Y$ and $X-S$ directions increase evidently, indicating the increasing of the interchain coupling. The effects of the pressure for the gaps between the filled and the unfilled bands are different for different points in the Brillouin zone. The gaps at Z, U, and S change little with the increasing pressure. Both gaps at X and Y points are enlarged evidently at high pressure by a rate of 0.174 eV/GPa at X and of 0.191 eV/GPa at Y for GGA. The corresponding values for LDA are 0.093 eV/GPa and 0.106 eV/GPa. Different results are obtained at Γ point for GGA and LDA. Both gaps are enlarged by pressure, but with a rate of

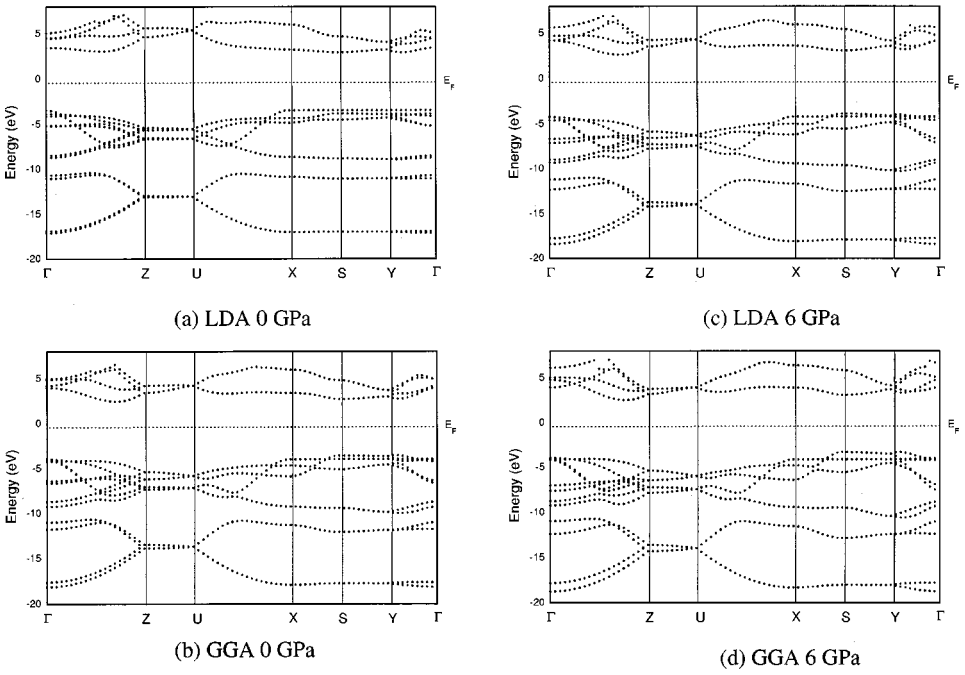

FIG. 2. LDA and GGA band structures of the polyethylene crystal for both 0 GPa and 6 GPa external pressure. (a) LDA, 0 GPa; (b) GGA, 0 GPa; (c) LDA, 6 GPa, and (d) GGA, 6 GPa.

TABLE VIII. Band characteristics of crystalline polyethylene under 0 GPa and 6 GPa external pressure, calculated by both LDA and GGA exchange-correlation potential. For comparison, a single chain LDA, a HF and the experimental results are listed together. Each value is in eV.

	GGA (0 GPa)	LDA (0 GPa)	GGA (6 GPa)	LDA (6 GPa)	LDA (single chain)[a]	HF[b]	Expt.
Gap	6.2	6.7	6.7	6.5	8.0	13.8	8.8
Total valence bandwidth	13.7	14.2	14.2	14.6	14.0	19.3	16.2
Low lying bandwidth	7.1	8.1	7.7	8.1	6.1	⋯	7.2
Gap	1.9	1.5	1.7	1.4	2.2	⋯	2.0
Upper two	4.7	4.6	4.8	5.1	5.3	⋯	6.7

[a]Reference 21.
[b]Reference 12.

0.247 eV/GPa for GGA and only a rate of 0.012 eV/GPa for LDA. In comparison with the covalent semiconductors, these pressure coefficients are considerably large. For example, the Γ gap pressure coefficient is calculated to be 0.049 eV/GPa by a LAPW method using LDA.[56]

VII. CONCLUSIONS

In this article, the geometry, elastic moduli and band structures of the crystalline polyethylene are studied by a pseudopotential plane wave method as a function of applied pressure. Both LDA and GGA exchange-correlation potential and energy are used. The GGA corrects the LDA interchain parameters, including interchain atomic distances and the lattice constants, and gives very good geometry parameters in comparison with the experiments. No evident correction of the band structures is found by GGA. Both GGA and LDA give good elastic modulus along the chain direction in comparison with the experiments but show deficiencies on the modulus concerning with the interchain interactions. Although GGA produces better geometry, it is hard to conclude that it describes the intermolecular interactions qualitatively better than LDA. Both LDA and GGA bands are in good agreements with the previous theoretical results of crystal as well as single chains. The general deficiency of LDA and GGA on band gaps does not show off manifestly and the calculated gap is close to the optical gap. The pressure shows a very large effect on the gaps, especially at Γ, X, Y points.

ACKNOWLEDGMENTS

Two of the authors, (M.S.M. and V.E.V.D.) are supported partly under Grants Nos. G2131.94 and G0347.97 of the Belgian National Science Foundation (NFWO) and partly by the Concerted Action of the University of Antwerpen on ''Influence of electron correlation on properties of biomolecules and the performance using density functional theory.'' J.L.M. was supported by Grant No. PRAXIS/PCEX/FIS/11213/98.

[1] H. Tadokoro, *Structure of Crystalline Polymers* (Wiley, New York, 1979).
[2] J. J. Ladik, *Quantum Theory of Polymers as Solids* (Plenum, New York, 1988).
[3] Jean-Marie André, Joseph Delhalle, and Jean-Luc Brédas, *Quantum Chemistry Aided Design of Organic Polymers* (World Scientific, Singapore, 1991).
[4] W. L. McCubbin and R. Manne, Chem. Phys. Lett. **2**, 230 (1968).
[5] R. L. MuCullough, J. Macromol. Sci. B **9**, 97 (1974).
[6] P. G. Perkins, A. K. Marhara, and J. J. P. Stewart, Theor. Chim. Acta **57**, 1 (1980).
[7] A. Imamura, J. Chem. Phys. **52**, 3168 (1970).
[8] H. Fujita and A. Imamura, J. Chem. Phys. **53**, 4555 (1970).
[9] K. Morokuma, Chem. Phys. Lett. **6**, 186 (1970).
[10] K. Morokuma, J. Chem. Phys. **54**, 962 (1971).
[11] J. M. André, J. Delhalle, S. Delhalle, R. Caudano, J. J. Pireaux, and J. Verbist, J. Chem. Phys. **60**, 595 (1974).
[12] A. Karpfen, J. Chem. Phys. **75**, 238 (1981).
[13] A. Karpfen and A. Beyer, J. Comput. Chem. **5**, 11 (1984).
[14] J. M. André, D. P. Vercauteren, V. P. Bodart, and J. G. Fripiat, J. Comput. Chem. **5**, 535 (1984).
[15] H. Teramae, T. Yamabe, and A. Imamura, Theor. Chim. Acta **64**, 1 (1983).
[16] S. Suhai, J. Polym. Sci., Polym. Phys. Ed. **21**, 1341 (1983).
[17] S. Suhai, J. Chem. Phys. **84**, 5071 (1986).
[18] J. E. Falk and R. J. Fleming, J. Phys. C **6**, 2954 (1973).
[19] R. V. Kasowski, W. Y. Hsu, and E. B. Caruthers, J. Chem. Phys. **72**, 4896 (1980).
[20] M. Springborg and M. Lev, Phys. Rev. B **40**, 3333 (1989).
[21] M. S. Miao, P. E. Van Camp, V. E. Van Doren, J. J. Ladik, and J. W. Mintmire, Phys. Rev. B **54**, 10430 (1996).
[22] P. Vogl and D. K. Campbell, Phys. Rev. B **41**, 12797 (1990).
[23] C. Ambrosch-Draxl, J. A. Majewski, P. Vogl, and G. Leising, Phys. Rev. B **51**, 9668 (1995).
[24] B. Montanari and R. O. Jones, Chem. Phys. Lett. **272**, 347 (1997).
[25] J. C. L. Hageman, R. J. Meier, M. Heinemann, and R. A. de Groot, Macromolecules **30**, 5953 (1997).
[26] J. C. L. Hageman, R. A. de Groot, and R. J. Meier, Comput. Mater. Sci. **10**, 180 (1998).
[27] I. Souza and J. L. Martins, Phys. Rev. B **55**, 8733 (1997).
[28] D. M. Ceperley and B. J. Alder, Phys. Rev. Lett. **45**, 566 (1980).
[29] J. P. Perdew and A. Zunger, Phys. Rev. B **23**, 5048 (1981).
[30] J. P. Perdew, K. Burke, and M. Ernzerhof, Phys. Rev. Lett. **77**, 3865 (1996); J. P. Perdew, K. Burke, and Y. Wang, Phys. Rev. B **54**, 16533 (1996).
[31] N. Troullier and J. L. Martins, Phys. Rev. B **43**, 1993 (1991).
[32] P. R. Vansant, P. E. Van Camp, V. E. Van Doren, and J. L. Martins, Phys. Rev. B **57**, 7615 (1998).
[33] C. W. Bunn, Trans. Faraday Soc. **35**, 482 (1939).
[34] S. Kavesh and J. M. Schultz, Polym. Sci. Part **A-2**, 8243 (1970).
[35] G. Avitabile, R. Napolitano, B. Pirozzi, K. D. Rouse, M. W. Thomas, and B. T. M. Willis, J. Polym. Sci., Polym. Lett. Ed. **13**, 351 (1975).
[36] G. König and G. Stollhoff, J. Chem. Phys. **91**, 2993 (1989).
[37] B. Champagne, J. G. Fripiat, and J. M. André, Phys. Mag. **14**, 123 (1992).
[38] A. D. Becke, Phys. Rev. A **38**, 3098 (1988).
[39] J. P. Perdew, Phys. Rev. B **33**, 8822 (1986).
[40] O. H. Nielsen and R. M. Martin, Phys. Rev. **32**, 3780 (1985).
[41] O. H. Nielsen and R. M. Martin, Phys. Rev. **32**, 3792 (1985).
[42] L. C. Blabás, J. L. Martins, and J. Soler (to be published).
[43] M. J. S. Dewar, Y. Yamaguchi, and S. Huck, Chem. Phys. **43**, 145 (1979).
[44] A. L. Brower, J. R. Sabin, B. Crist, and M. A. Ratner, Int. J. Quantum Chem. **18**, 651 (1980).
[45] B. Crist and P. G. Hereña, J. Polym. Sci. Polym. Phys. **34**, 449 (1996).
[46] M. L. Zhang, M. S. Miao, V. E. Van Doren, A. Peeters, C. Van Alsenoy, J. J. Ladik, and J. W. Mintmire, Solid State Commun. **116**, 339 (2000).

[47] A. Peeters, C. Alsenoy, M. L. Zhang, and V. E. Van Doren, Int. J. Quantum Chem. **80**, 425 (2000).
[48] I. Sakurada, U. Nukushina, and T. Ito, J. Polym. Sci. **57**, 651 (1962).
[49] R. A. Feldkamp, G. Venkaterman, and J. S. King, *Neutron Inelastic Scattering* (IAEA, Vienna, 1968), Vol. 2, p. 159.
[50] R. G. Schaufele and T. Schimanouchi, J. Chem. Phys. **42**, 2605 (1967).
[51] J. Barham and A. Koller, J. Polym. Sci., Polym. Lett. Ed. **17**, 591 (1979).
[52] Y. Zhao, J. Wang, Q. Cui, Z. Liu, M. Yang, and J. Shen, Polymer **31**, 1425 (1990).
[53] D. J. Lacks, J. Phys. Chem. **99**, 14430 (1995).
[54] K. Seki, N. Ueno, U. O. Karsson, R. Engelhardt, and E.-E. Koch, Chem. Phys. **105**, 247 (1986).
[55] H. Fujimoto, T. Mori, H. Inokuchi, N. Ueno, K. Sugita, and K. Seki, Chem. Phys. Lett. **141**, 485 (1987).
[56] Su-Huai Wei and Alex Zunger, Phys. Rev. B **60**, 5404 (1999).